THE JOURNAL OF PHYSICAL CHEMISTRY A

 VOLUME 110, NUMBER 19, MAY 18, 2006

ARTICLES

Excited-State Structural Dynamics of 5-Fluorouracil

Brant E. Billinghurst, Ralph Yeung, and Glen R. Loppnow*

Department of Chemistry, University of Alberta, Edmonton, Alberta T6G 2G2, Canada

Received: February 13, 2006; In Final Form: March 17, 2006

5-Fluorouracil is an analogue of thymine and uracil, nucleobases found in DNA and RNA, respectively. The photochemistry of thymine is significant; UV-induced photoproducts of thymine in DNA lead to skin cancer and other diseases. In previous work, we have suggested that the differences in the excited-state structural dynamics of thymine and uracil arise from the methyl group in thymine acting as a mass barrier, localizing the vibrations at the photochemical active site. To further test this hypothesis, we have measured the resonance Raman spectra of 5-fluorouracil at wavelengths throughout its 267 nm absorption band. The spectra of 5-fluorouracil and thymine are very similar. Self-consistent analysis of the resulting resonance Raman excitation profiles and absorption spectrum using a time-dependent wave packet formalism suggests that, at most, 81% of the reorganization energy upon excitation is directed along photochemically relevant modes. This compares well with what was found for thymine, supporting the mass barrier hypothesis.

Introduction

Deoxyribonucleic acid (DNA), which stores genetic information, and ribonucleic acid (RNA), which mediates translation of the genetic code into proteins, are composed of two purines, adenine and guanine, and three pyrimidines, cytosine, thymine, and uracil.[1] Thymine is present only in DNA, while uracil only appears in RNA.

Interest in thymine and uracil arises from the fact that, even though they only differ structurally by a methyl group in the 5-position (Scheme 1), large differences are observed in their resonance Raman spectra (see below). The photochemistry of thymine and uracil dinucleotides (TpT and UpU, respectively) is also very different (Scheme 2).[2] Thymine dinucleotides preferentially form the cyclobutane pyrimidine dimer (CPD) with a quantum yield, $\phi = 0.013$, as a result of [2 + 2]-cycloaddition between the C═C bonds of adjacent thymines or the [6−4] photoproduct ($\phi = 0.003$) as a result of [2 + 2]-cycloaddition between the C═C bond of one thymine and the C═O bond of the adjacent thymine. Uracil dinucleotides form the photohydrate ($\phi = 0.018$) as the major photoproduct and the CPD ($\phi = 0.007$).[2] The photohydrate is the result of solvent addition across the C═C bond.

SCHEME 1

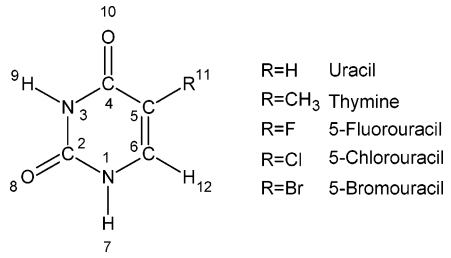

A probe for the initial excited-state structural dynamics is crucial to understanding the photochemistry of the nucleobases. Resonance Raman spectroscopy is a powerful probe of excited-state molecular structure and initial dynamics.[3] By tuning the exciting laser into the absorption band, resonant enhancement of those vibrational modes coupled to the electronic excitation

* To whom correspondence should be addressed. E-mail: glen.loppnow@ualberta.ca.

10.1021/jp0609333 CCC: $33.50
Published on Web 04/25/2006

SCHEME 2

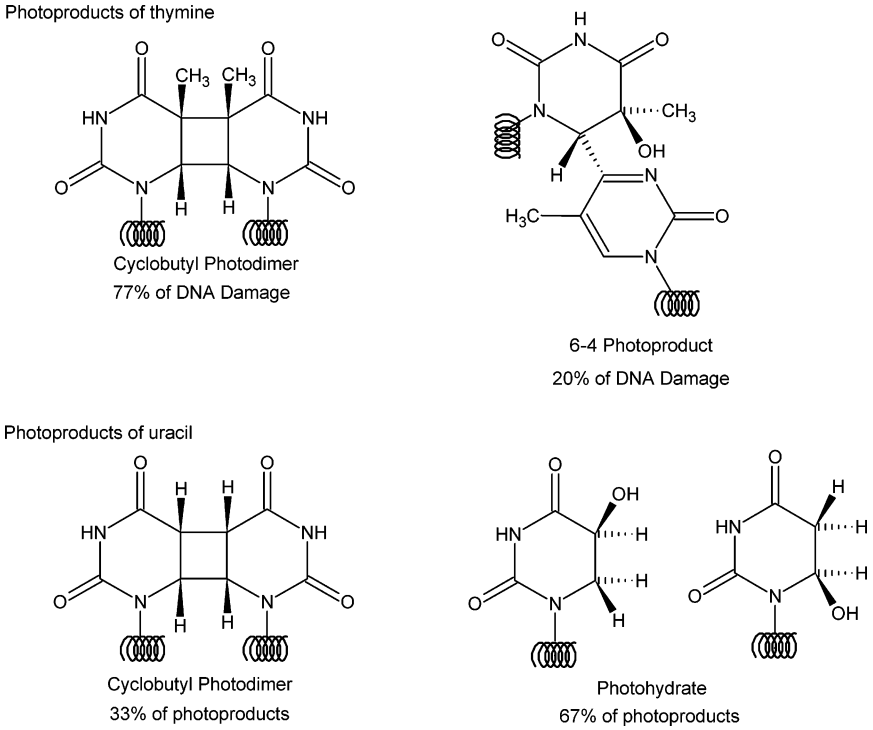

occurs. The resonance Raman vibrational band intensity is directly proportional to the slope of the excited-state potential energy surface along that vibrational coordinate; the greater the change in the molecular structure along the vibrational coordinate, the more intense the resulting resonance Raman band will be. Thus, the intensities of the resonance Raman bands will directly reflect the conformational distortion of the molecule along each of the normal mode coordinates in the excited state.[4]

Previous[5] analysis of the resonance Raman excitation profiles and absorption spectra for thymine and uracil within the 266 nm absorption band showed that their excited-state structural dynamics were significantly different. It was found that thymine had 73% of its reorganization energy directed along photochemically relevant modes, while uracil had only 13% of its reorganization energy directed along photochemically relevant modes.[5] It was postulated[5] that the methyl group in thymine acts as a mass barrier and localizes the reorganization energy along photochemically relevant vibrational modes.

Here, we further test this model by measuring the excited-state structural dynamics of 5-fluorouracil. Fluorine in the 5-position has a mass similar to the methyl group in thymine but has very different electronic, steric, and vibrational coupling properties. The fluoro group does not directly change the electronic transition since the 265 nm absorption maximum is the same in 5-fluorouracil and thymine. However, it is reasonable to suspect that the number and energies of intervening "dark" states and the energies of the states involved in the transition may be affected by the substitution of a fluorine for a methyl group. Furthermore, it has been shown by Mathies et al. that methyl groups can vibrationally couple to adjacent carbon−carbon double bonds in retinals.[6] Therefore, this pyrimidine analogue is optimal for testing the effect of the 5-substituent mass on the excited-state structural dynamics. The results obtained here demonstrate that the resonance Raman spectrum and excited-state structural dynamics of 5-fluorouracil are similar to those of thymine. These observations support the mass barrier model as a determinant of pyrimidine nucleobase excited-state structural dynamics.

Experimental Section

5-Fluorouracil (2,4-dioxo-5-fluoropyrimidine), 5-chlorouracil, 5-bromouracil (99%, Sigma, Oakville, Ontario), and sodium sulfate (99%, EMD Chemicals Inc., Gibbstown, NJ) were obtained commercially and used without further purification. All samples were prepared using Nanopure water from a Barnstead water filtration system (Boston, MA).

Laser excitation for the resonance Raman experiments was obtained using a picosecond mode-locked Ti:sapphire laser (Coherent, Santa Clara, CA) pumped with a Verdi V-10 diode-pumped laser (Coherent, Santa Clara, CA). To obtain the 244, 257, 266, 275, and 290 nm wavelengths, the output of the Ti:sapphire was doubled using a lithium triborate (LBO) crystal followed by third-harmonic generation in a β-barium borate (β-BBO) crystal (Inrad, Northvale, NJ). Typical laser powers were 2−20 mW. The resulting laser beam was spherically focused on an open stream of flowing solution in a 135° backscattering geometry. All the resonance Raman spectra were obtained using 1.6 mM 5-fluorouracil solutions containing 0.3 M sodium sulfate internal standards. Resonance Raman spectra were collected for 5-chlorouracil and 5-bromouracil at an excitation wavelength of 275 nm in the same manner. The addition of sodium sulfate as an internal standard had no noticeable effect on either the absorption or resonance Raman spectra of any of the 5-halouracils. The resonance Raman scattering was focused into a double-grating spectrophotometer with a diode array detector. The laser system and spectrometer have been described in detail previously.[7] Measurements of the resonance Raman spectra and determinations of intensities were repeated on three fresh samples of 5-fluorouracil at each wavelength. Frequency calibration was performed by measuring the Raman scattering of organic solvents for whom the peak positions are known (*n*-pentane, cyclohexane, dimethylformamide, ethanol, acetonitrile, and acetic acid). Frequencies are accurate to ± 2 cm^{-1}. Analysis of the data was performed as previously described.[5,7,8] Absorption spectra were acquired before and after each Raman scan using a diode array spectrometer (Hewlett-Packard, model

8452A, Sunnyvale, CA). No significant change in absorbance was observed, suggesting that a bulk photoalteration parameter below 5% was observed.[9]

The 257 nm excited resonance Raman spectrum of 5-fluorouracil in the overtone and combination band region was recorded using the same system as described for the fundamental region, except that the 1705 cm^{-1} band of 5-fluorouracil was used to calculate the resonance Raman cross sections. Also, 0.2 M acetonitrile was added to provide a common peak in both spectral windows. Acetonitrile had no effect on the absorption or resonance Raman spectra.

The methods used for converting the resonance Raman intensities of 5-fluorouracil into absolute cross sections and for self-absorption correction have been described previously.[5,7,8,10,11] The experimental differential Raman cross sections for sulfate used in this work were 3.23×10^{-12}, 2.47×10^{-12}, 2.08×10^{-12}, 1.77×10^{-12}, and 1.35×10^{-12} $Å^2$/(molecule sr) at 244, 257, 266, 275, and 290 nm, respectively. Depolarization ratios of 0.33 and 0.05 were used for 5-fluorouracil and sulfate, respectively.

Theory

The resonance Raman excitation profiles were simulated with the time-dependent wave packet formalism expressed by the following equations[4,12]

$$\sigma_R(E_L) = \frac{8\pi E_S{}^3 E_L e^4 M^4}{9\hbar^6 c^4} \int_0^\infty dE_0\, H(E_0) \left| \int_0^\infty dt\, \langle f|i(t)\rangle \exp\left\{\frac{i(E_L + \epsilon_i)t}{\hbar}\right\} G(t)\right|^2 \quad (1)$$

$$\sigma_A(E_L) = \frac{4\pi E_L e^2 M^2}{6\hbar^2 cn} \int_0^\infty dE_0\, H(E_0) \int_{-\infty}^\infty dt\, \langle i|i(t)\rangle \exp\left\{\frac{i(E_L + \epsilon_i)t}{\hbar}\right\} G(t) \quad (2)$$

where E_L and E_S are the energies of the incident and scattered photons, respectively, M is the transition length, n is the refractive index, ϵ_i is the energy of the initial vibrational state, $H(E_0)$ is a normalized inhomogeneous distribution of zero−zero energies around an average energy ($\bar{E}_0$) expressed as

$$H(E_0) = (2\pi\theta)^{-1/2} \exp\left\{\frac{-(\bar{E}_0 - E_0)^2}{2\theta^2}\right\} \quad (3)$$

where θ is the standard deviation of the distribution, $|i\rangle$ and $|f\rangle$ are the initial and final vibrational wave functions in the Raman process, $|i(t)\rangle$ is the initial ground-state vibrational wave function propagated on the excited-state potential energy surface, and $G(t)$ is the homogeneous line width function. Within the separable harmonic oscillator approximation, the $\langle i|i(t)\rangle$ and $\langle f|i(t)\rangle$ overlaps are significantly sensitive only to the differences in ground- and excited-state equilibrium geometries along each normal mode (Δ). Thus, the resonance Raman intensities directly reflect the dynamics of the excited state.

For molecules interacting with a bath, $G(t)$ represents the dynamics of the chromophore−solvent coupling. The solute−solvent interactions that contribute to the solvent-induced homogeneous broadening are modeled using the Brownian oscillator model developed by Mukamel and co-workers.[13] The general implementation of these equations for absorption and resonance Raman spectroscopy has been described in detail previously.[14,15] In our analysis we assume that the system remains within the strongly damped and high-temperature ($h\Lambda \ll kT$) limits.

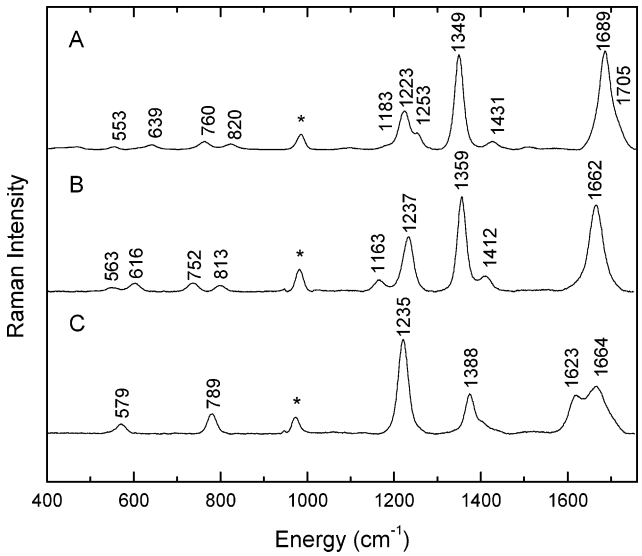

Figure 1. Resonance Raman spectra of 1.6 mM 5-fluorouracil (A), 3 mM thymine[5] (B), and 3 mM uracil[5] (C) in water excited at 266 nm. The bands due to the internal standards (0.3 M sodium sulfate for 5-fluorouracil and 0.4 M sodium sulfate for uracil and thymine) are indicated by asterisks (*). The peak that appears near 1500 cm^{-1} in 5-fluorouracil was not reproducible at all excitation wavelengths and is therefore not considered in this paper.

The initial guesses for the displacements along each normal coordinate (Δ) were based on the assumption that the average relative resonance Raman intensities are proportional to Δ^2, with the intensity of the 1689 cm^{-1} mode arbitrarily set to 1. The relative Δ's were scaled to reproduce the experimentally observed absorption and resonance Raman excitation profile bandwidths. All 11 observed fundamental modes were included in the time-dependent calculations. Overtone vibrations below 3500 cm^{-1} were further used to constrain the simulation. The parameters were then optimized iteratively as described previously[15] until the best possible agreement was obtained between the calculated and experimental absorption spectra and resonance Raman excitation profiles.

Results

The resonance Raman spectra of 5-fluorouracil, thymine, and uracil are shown in Figure 1. The spectra of 5-fluorouracil show no frequency shifts or relative intensity changes at different excitation wavelengths within the 267 nm absorption band. This result indicates that the Raman spectra are enhanced by a single electronic transition. Eleven bands are observed between 500 and 1700 cm^{-1} for 5-fluorouracil. These bands have been assigned on the basis of potential energy distributions (PED) given by Dobrowolski et al. derived from DFT calculations at the B3PW91/6-311G** level of theory.[16] The observed good agreement between the calculated and observed frequencies[16] suggests that the PED's are accurate. The assignments given in Table 1 are the ones that offer the best match between experimental and calculated frequencies and intensities.

The 1689 cm^{-1} band is the most intense band found in 5-fluorouracil and is assigned as $\nu(C_5{=}C_6)$. This band strongly overlaps the 1705 cm^{-1} band, which is assigned to $\nu(C_4{=}O)$.[16] The band at 1349 cm^{-1} is also very intense and is assigned to the $\beta(C_6{-}H_{12}) + \nu$(ring) mode.[16] Comparing the spectrum of 5-fluorouracil to those of thymine and uracil, it is immediately

TABLE 1: Raman Frequencies, Assignments, and Harmonic Parameters for 5-Fluorouracil (Bold Entries Are Photochemically Relevant Modes)

mode[a] (cm^{-1})	assignment and PED %[b]	$\|\Delta\|$[c]	E[d] (cm^{-1})
1705	$78\nu(C_4{=}O)$	0.33	93
1689	$\mathbf{71\nu(C_5{=}C_6)}$	**0.85**	**610**
1431	$29\nu[(N_1{-}C_2){-}(C_2{-}N_3){-}(N_3{-}C_4)+(C_4{=}O_{10})]+21\beta(N_1{-}H_7){-}11\beta^{as}(C{=}O)$	0.26	48
1349	$\mathbf{46\beta(C_6{-}H_{12})+16\nu[(N_1{-}C_2){-}(C_2{-}N_3)+(N_3{-}C_4){-}(C_4{-}C_5){+}(C_5{=}C_6)]+11\nu[(C_4{-}C_5){-}(N_1{-}C_2)]}$	**0.75**	**379**
1253	$44\nu(C_5{-}F_{11})+14\nu[(N_1{-}C_2){-}(C_2{-}N_3){-}(N_3{-}C_4)+(C_4{=}O_{10})]+14\beta[(C_4C_5C_6){-}(N_1C_2N_3)]$	0.29	53
1223	$\mathbf{41\nu[(N_1{-}C_2){-}(C_2{-}N_3)+(N_3{-}C_4){-}(C_4{-}C_5){+}(C_5{=}C_6)]{-}21\beta\,(C_6{-}H_{12})+11\nu^{as}(CN)}$	**0.47**	**135**
1183	$45\nu^{as}(CN)+18\beta\,(N_1{-}H_7)$	0.20	24
820	$57\beta[(C_4C_5C_6){-}(N_1C_2N_3)]{-}16\nu(C_5{-}F_{11})$	0.19	14
760	$83\gamma(C_2{=}O_8){-}13\gamma(C_4{=}O_{10})$	0.21	17
639	$86\gamma(N_3{-}H_9)$	0.15	7.2
553	$94\gamma(N_1{-}H_7)$	0.11	3.3

[a] Frequencies listed are the experimental frequencies reported here. [b] Abbreviations: ν is stretching, γ is out-of-plane bending, β is in-plane bending, and superscript "as" is asymmetric. The numbers represent the percentage PED of that internal coordinate in the mode. Assignments are from ref 16. Only the internal coordinates with percentages larger than 10% are listed. [c] Displacements (Δ) are in units of dimensionless normal coordinates and were obtained by fitting eqs 1 and 2 with the following parameters: temperature $T = 298$ K, Brownian oscillator line shape $\kappa = \Lambda/D = 0.1$, Gaussian homogeneous line width $\Gamma_G = 650$ cm^{-1}, inhomogeneous line width $\theta = 1300$ cm^{-1}, zero−zero energy $E_0 = 36\,212$ cm^{-1} and transition length $M = 0.61$ Å. The estimated errors in the parameters used in the calculation are as follows: $E_0 \pm 1\%$, $M \pm 1\%$, $\Gamma \pm 5\%$, $\theta \pm 5\%$, and $\Delta \pm 5\%$. [d] E is the reorganization energy calculated using eq 4.

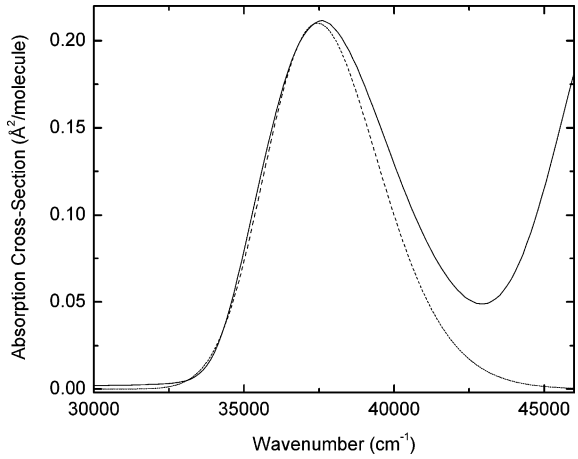

Figure 2. Experimental (solid line) and simulated (dotted line) absorption spectra of 5-fluorouracil. The simulated absorption spectrum was calculated using eq 2 with the parameters in Table 1. Discrepancies observed above 38000 cm^{-1} are due to higher energy electronic transitions which were not modeled here.

clear that the 5-fluorouracil spectrum bears a striking resemblance to that of thymine and much less to that of uracil. In fact, similarities between the 5-fluorouracil and the thymine spectra are remarkable in that both have four weak peaks between 500 and 900 cm^{-1} and both have very intense peaks at ~1350 and 1680 cm^{-1}. The only major difference between the spectra is found in the 1100−1300 cm^{-1} region. This result is not surprising, as the 1253 cm^{-1} band in 5-fluorouracil involves the C−F stretch, while the 1237 cm^{-1} band in thymine involves the $C{-}CH_3$ stretch.

The experimental and simulated absorption spectra are shown in Figure 2, while the experimental and simulated resonance Raman profiles are shown in Figure 3. Figures 2 and 3 show good agreement between the experimental and calculated resonance Raman profiles and absorption spectra. Deviations between the experimental and calculated absorption spectra which appear above 38 000 cm^{-1} are attributed to higher energy electronic transitions which are not modeled here. The different relative Raman intensities of the vibrational bands seen in Figure 1 are directly reflected in the different experimental Raman cross sections (Figure 3) and excited-state geometry displacements (Table 1).

To better constrain the parameter set which accurately describes the absorption spectra and fundamental resonance Raman excitation profiles, the overtones and combination bands between 1700 and 2900 cm^{-1} were also measured at 257 nm.

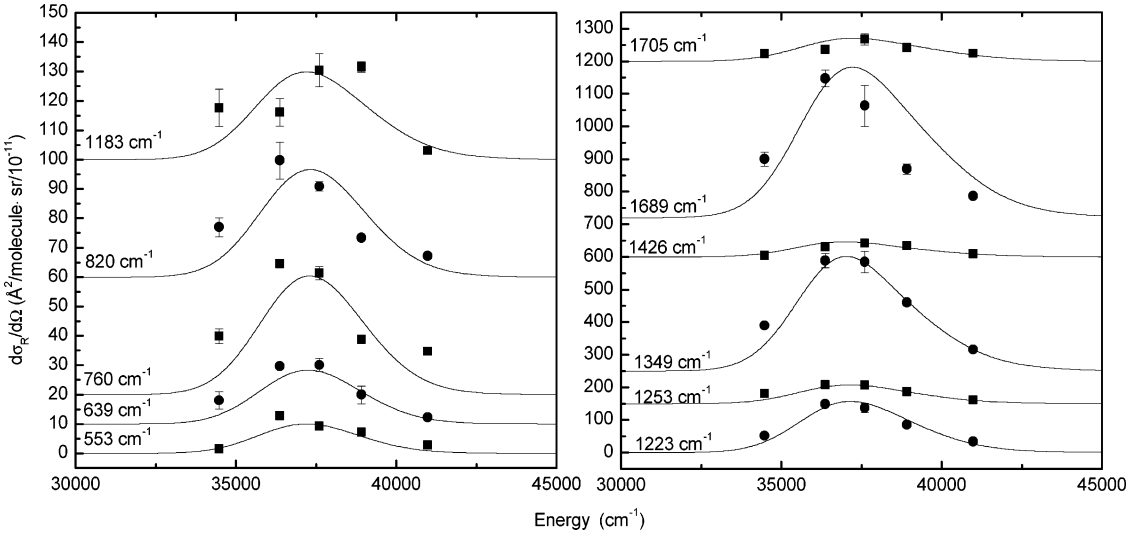

Figure 3. Experimental (points) and calculated (solid line) resonance Raman excitation profiles of 5-fluorouracil. The excitation profiles were calculated with eq 1 with the parameters in Table 1. The excitation profiles have been offset along the ordinate for greater clarity of presentation.

TABLE 2: Experimental and Calculated Absolute Resonance Raman Overtone and Combination Band Cross Sections for Cytosine[a]

mode (cm^{-1})	exptl $d\sigma_R/d\Omega$ ($Å^2$/(molecule sr)/10^{-11})	exptl $d\sigma_R/d\Omega$ ($Å^2$/(molecule sr)/10^{-11})
1981	11 ± 0.2	5 ± 0.5
2106	9 ± 1	10 ± 1
2162	8 ± 1	9 ± 1
2444	18 ± 4	14 ± 1
2567	28 ± 4	22 ± 2
2638	1 ± 0.1	1 ± 0.1

[a] The excitation wavelength is 257 nm. Cross sections were calculated with eq 1 by using the parameters of Table 1. [b] The error values stated are estimated from the error in the parameters and the consequent variability in the goodness of fit.

Although some overtones are expected at frequencies greater than 3000 cm^{-1}, these were obscured by the broad O−H stretching vibrations of water. It is well-known that the overtone and combination band intensities are more sensitive to the excited-state geometry displacements (Δ's) and provide an additional constraint on the excited-state parameters. The experimental and calculated cross sections for all of the observed overtones and combination bands of uracil and thymine are given in Table 2. The calculated cross sections from the parameters in Table 1 are all within the experimental error of the experimental cross sections, suggesting that these parameters accurately reflect the excited-state structural dynamics of 5-fluorouracil. The one exception is the 1981 cm^{-1} mode, composed of the 639 + 1349 cm^{-1} modes. This discrepancy is probably due to the observed band reflecting the intensity of several overlapping combination bands, which may fall in that region such as the 553 + 1426 cm^{-1} and the 760 + 1223 cm^{-1} combination bands.

The resonance Raman spectra of 5-chlorouracil and 5-bromouracil at an excitation wavelength of 275 nm are compared with that of 5-fluorouracil in Figure 4. The spectra of all three halouracils are very similar. The major difference between the halouracil spectra is that the C═C stretch band is shifted from 1689 cm^{-1} in 5-fluorouracil to ∼1630 cm^{-1} in 5-bromo- and 5-cholorouracil, while the C═O stretch remains at approximately the same frequency, decreasing the overlap between the bands. The spectra of 5-bromouracil and 5-chlorouracil are essentially the same.

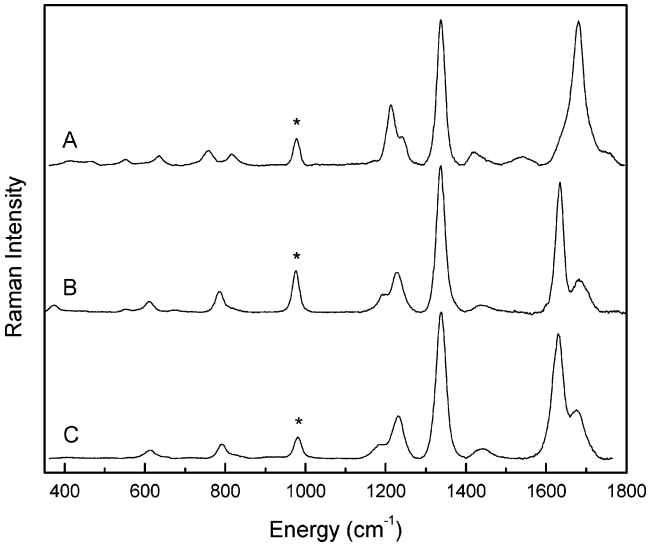

Figure 4. Resonance Raman spectra of 1.6 mM 5-fluorouracil (A), 5-chlorouracil (B), and 5-bromouracil (C) in water excited at 275 nm. The band due to the internal standard (0.3 M sodium sulfate) in each spectrum is indicated by an asterisk (*).

Discussion

Photochemical Structural Dynamics. In understanding the excited-state structural dynamics of 5-fluorouracil, it is helpful to first consider the photochemistry of 5-fluorouracil. Previous work has shown that only the photohydrate was observed in the photochemistry of free 5-fluorouracil nucleobase.[17] Some photodimerization is observed in the presence of an acetone or *N*-methyllutidone photosensitizer, suggesting that the triplet state leads to the photodimer in the 5-fluorouracil nucleobase, similar to that observed for thymine and uracil nucleobases in solution. Although the photochemistry of 5-fluorouracil dinucleotides has not been measured, two papers have reported the photochemistry of butyl-linked 5-fluorouracil nucleotides. In both cases, the photohydrate was the dominant product. In those papers it was also noted that the cyclobutyl photodimer forms in the presence of an acetone sensitizer.[18,19] Thus, the photochemistry of 5-fluorouracil appears to be localized around the C_5═C_6 bond. Experiments are currently underway in our group to measure the photochemistry of the 5-fluorouracil dinucleotides.

Considering the above photochemistry and that the resonance Raman intensity is roughly proportional[4] to Δ^2, one can predict which vibrational modes will have resonance Raman intensity. This prediction assumes that the initial excited-state structural dynamics lie along the photochemical reaction coordinate. For the formation of either the photodimer or the photohydrate, there are two significant changes that occur during the photochemical reaction. One is that the C_5═C_6 double bond becomes a single bond. Therefore, one would expect to see intense resonance Raman bands for modes that involve the C═C stretch. Also, the hybridization of the C_5 and C_6 carbons goes from sp^2 to sp^3. Therefore, modes involving either CH or CF bending, deformation, or wagging on those carbons would be expected to have significant intensity.

We correlated the resonance Raman active modes of 5-fluorouracil listed in Table 1 to the modes that are photochemically relevant. Three modes are found to be photochemically relevant: the 1689 cm^{-1} band which is mostly $\nu(C_5{=}C_6)$, the 1349 cm^{-1} band which contains both $\beta(C_6{-}H_{12})$ and $\nu(C_5{=}C_6)$, and the 1223 cm^{-1} mode which involves $\beta(C_6{-}H_{12})$ (Table 1). It is important to note that these three modes also have the largest Δ's observed.

Using these assignments and the relation

$$E = \Delta^2\tilde{\nu}/2 \tag{4}$$

the reorganization energy, E, can be calculated from the frequencies ($\tilde{\nu}$) and Δ's given in Table 1. Taking the sum of all of the photochemically relevant modes (bold, Table 1) as a percentage of the total reorganization energy for all of the modes, we see that 81% of the reorganization energy involved in the transition occurs along photochemically relevant modes. This result can be considered as an upper limit for the percentage of reorganization energy directed along the photochemically relevant coordinates. By scaling the reorganization energy in the photochemically active modes by the percentage of the mode which is localized along a photochemically relevant coordinate, a lower limit for the percentage of reorganization energy along the photochemically relevant coordinate of 46% is obtained.

The displacement between the ground- and excited-state potential minima along a particular internal coordinate δ can be found using the following equation

$$\delta = 5.8065\sum A_{ij}\bar{\omega}_j^{-1/2}\Delta_j \tag{5}$$

where A_{ij} is the normal mode coefficients $\bar{\omega}_j$ is the mode's frequency and Δ_j is the dimensionless displacement. If we consider only the 1689 cm^{-1} $C_5{=}C_6$ stretching vibration and ignore any contributions from ring stretching modes, a change in the $C_5{=}C_6$ bond length of 0.085 Å is obtained in the excited state. This value is identical to the 0.08 Å obtained in the excited state for thymine[5] and compares favorably with the 0.14 Å obtained from a calculation of the transition-state structure in the formation of the thymidine cyclobutyl photodimer.[20]

Comparison with Thymine and Uracil. Comparing the spectra of 5-fluorouracil to those of thymine and uracil,[5] we can follow how the addition of either a methyl or fluoro group increases the amount of reorganization energy in photochemically relevant coordinates. In the 1600−1750 cm^{-1} region, the UV resonance Raman spectra of all three nucleobases contain 1−2 relatively strong peaks which can be assigned to the C═C stretch or the C═O stretch. In uracil, the C═O stretch has a higher frequency and Δ than the C═C stretch, whereas the reverse is true for 5-fluorouracil and probably for thymine. Because the modes overlap for thymine, we cannot definitively extend this argument to it. In the spectra of 5-chloro and 5-bromouracil the C═C stretching frequency has decreased enough to resolve the C═O stretch, demonstrating that the C═C stretching band is significantly more intense than the C═O stretching band. This offers evidence that the curve-fit analysis done for 5-fluorouracil was indeed correct in assigning more of the intensity to the C═C stretch. In both thymine and 5-fluorouracil, there is a very strong peak at ∼1350 cm^{-1} that is assigned to $C_6{-}H_{12}$ bending and a weak peak which is assigned to some combination of ring stretching and $N_1{-}H_7$ bend. However, the strong peak observed in this region in uracil is assigned to a more delocalized ring stretching vibration.[5] In the 1200−1300 cm^{-1} region, only a single strong peak is observed for uracil, assigned to a delocalized ring stretching mode. For both 5-fluorouracil and thymine, there are two medium-intensity peaks in this region: one involving the stretching mode of the C_5 substituent and one involving $C_6{-}H_{12}$ bending. For 5-fluourouracil, a large amount of ring stretching is also observed with the $C_6{-}H_{12}$ bending.[5] Thus, all these results suggest that thymine and 5-fluorouracil contain larger excited-state structural distortions along the photochemical C═C bond, supporting the model that a massive substituent on C_5 localizes the excited-state reorganization energy around the photochemically active site.

Comparing the amount of reorganization energy along photochemically relevant modes, the 81% found for 5-fluorouracil is much closer to the 73% found for thymine than the 13% found for uracil.[5] If the excited-state structural dynamics are the only determinant of the photochemistry, this result would suggest that the photochemistry of 5-fluorouracil should be more like thymine, i.e., preferentially forming the photodimer over the photohydrate in the dinucleotides. Since no work has been done on the photochemistry of the 5-fluorouracil dinucleotides, the correlation between photochemistry and excited-state structural dynamics is still unclear. However, because 5-fluorouracil appears to preferentially form the photohydrate when in a butyl linked dimer,[18,19] there may be other factors beyond the excited-state structural dynamics that influence the photochemistry of these systems. For example, the substituent on C_5 may affect the stacking of the nucleobases in the dinucleotides, change the character of the electronic excited state in the nucleobase, or alter the excited-state curve-crossing geometries and states.

Effect of the Halogen. The resonance Raman spectra of 5-fluoro-, 5-chloro-, and 5-bromouracil (Figure 4) are all very similar, suggesting that the excited-state structural dynamics for them are similar. This result is supported by the vibrational assignments and PEDs,[16] which are similar for all the halouracil modes discussed in this paper. The most noticeable difference between 5-fluorouracil and the other halouracils is that the C═C peak in the latter two is shifted to lower energy. This can be explained by the fact that X-ray structures show that the C═C bond length in the ground electronic state is longer in 5-bromouracil (1.355 Å) than in 5-fluorouracil (1.350 Å) and even longer in 5-chlorouracil (1.370 Å), suggesting that the halogen changes the ground-state structure of the molecule.[21−23] Furthermore, the addition of greater mass at C_5 should reduce the frequency of the C═C vibration through a reduced mass effect. Indeed, the C═C stretching frequency does decrease with increasing mass of the C_5 halogen. The photochemistry of both 5-chloro- and 5-bromouracil is different from that of either 5-fluorouracil or thymine as they both undergo photohomolytic cleavage of the $C_5{-}X$ bond.[24,25]

Broadening. Solvents may contribute significantly to the breadth of the absorption spectrum in the condensed phase through either inhomogeneous or homogeneous mechanisms. These two factors affect the observed absorption spectrum and resonance Raman excitation profiles differently. The inhomogeneous line width is due to ensemble "site" effects while the homogeneous line width represents contributions from excited-state population decay and pure dephasing. The relative contributions of these two broadening terms cannot be determined using the absorption spectrum alone as they both broaden the absorption spectrum. However, homogeneous broadening also dampens the resonance Raman excitation profile. For 5-fluorouracil, both the inhomogeneous and homogeneous line widths must be relatively large to reproduce the experimental absorption spectrum and resonance Raman excitation profiles.

Solvent-induced dephasing normally dominates homogeneous broadening in the condensed phase, although population decay may also contribute. To accurately model the magnitude of the resonance Raman cross sections and diffusiveness of the absorption spectrum, a Gaussian homogeneous line width of 650 cm^{-1} was required. Kohler et al. have determined the fluorescence lifetimes of pyrimidine thymine, uracil, and cytosine nucleosides, but not 5-fluorouracil, to be on the order of 290−720 fs.[26] Since the fluorescence lifetime and nonradiative rate constant are not known for 5-fluorouracil, the amount of homogeneous broadening that is due to population decay cannot be directly calculated. However, the excited-state lifetime required to cause the observed homogeneous broadening may be estimated. The observed absorption and resonance Raman spectra indicate that the line shape is primarily Gaussian. Thus, a 650 cm^{-1} line width yields a 1/e excited-state lifetime of 8 fs. This is much shorter than the lifetime of ∼1 ps observed for thymine and uracil.[2] It is known that for thymine and uracil population decay accounts for 3.5 cm^{-1} of the Gaussian line widths of 355 and 200 cm^{-1} respectively.[5] Therefore, it is reasonable to believe that the amount of homogeneous broadening due to population decay is relatively small compared to solvent-induced dephasing for 5-fluorouracil, as in thymine and uracil. Thus, most of the homogeneous line width observed for 5-fluorouracil is probably due to solvent-induced dephasing, as in thymine and uracil. This increased line width in 5-fluorouracil may be due to additional dipole−dipole interactions between the water molecules and the fluorine group. However, in the absence of fluorescence lifetime data for 5-fluorouracil, the possibility of an increase in the nonradiative decay rate cannot be completely dismissed.

Inhomogeneous broadening arises because there can be a number of different solvation structures in solution leading to a distribution of electronic transition energies. Inhomogeneous broadening is considered static on the time scale of the resonance Raman experiment. To accurately model the magnitude of the resonance Raman cross sections and diffuseness of the absorption spectrum, a Gaussian inhomogeneous line width of 1300 cm^{-1} was required. This is relatively close to the 1200 cm^{-1} inhomogeneous line width needed for thymine. This is reasonable, considering that thymine and 5-fluorouracil are structurally quite similar and therefore the solvation structures would also be expected to be quite similar. The slight increase seen for 5-fluorouracil might be due to an increased interaction between the fluoro group and the water molecules in comparison to a methyl group due to greater dipolar interactions compared to a methyl group.

Since an increase in both the solvent dephasing and inhomogeneous broadening is observed for 5-fluorouracil in comparison to thymine and uracil, it is clear that the addition of the fluoro group increases the interaction with the solvent. However, the increase in the homogeneous solvent-induced dephasing is much larger than the increase in the inhomogeneous broadening. This may indicate that the average range in solvation structures is not changed much but that there is a large change in the short time scale variability of the local environment. This may be because the fluoro group is a very strong electron-withdrawing group; therefore, any structural change involving the fluorine would cause significant changes in the interaction of the 5-fluorouracil molecule with the solvent.

Conclusions

The resonance Raman spectra and resulting analysis presented here provides insight into the excited-state structural dynamics and photochemistry of 5-fluorouracil as well as thymine and uracil. The three most intense bands observed for 5-fluorouracil found at 1689, 1349, and 1223 cm^{-1} are photochemically relevant. This leads to as much as 81% of the reorganization energy being directed along photochemically relevant coordinates. The excited-state structural dynamics for 5-fluorouracil are much more similar to those of thymine than for uracil. The resonance Raman spectra of all of the 5-halouracils observed were also very similar, with the most notable exception being the decrease in the C═C stretching frequency in 5-chloro- and 5-bromouracil compared to 5-fluorouracil. These results support the model that a massive substituent at C_5 localizes the excited-state structural dynamics at the photochemical active site.

Supporting Information Available: Figure 1S containing UV resonance Raman spectra of 5-fluorouracil with excitation wavelengths within the 267 nm absorption band. This material is available free of charge via the Internet at http://pubs.acs.org.

References and Notes

(1) Lehninger, A. L. *Biochemistry*; Worth Publications: New York, 1975; Vol. 2, pp 309−333.

(2) Ruzsicska, B. P.; Lemaire, D. G. E. In *CRC Handbook of Organic Photochemistry and Photobiology*; Horspool, W. H., Song, P.-S., Eds.; CRC Press: New York, 1995; pp 1289−1317.

(3) Fodor, S. P. A.; Rava, R. P.; Hays, T. R.; Spiro, T. G. *J. Am. Chem. Soc.* **1985**, *107*, 1520−1529.

(4) (a) Myers, A. B.; Mathies, R. A. In *Biological Applications of Raman Spectroscopy, Resonance Raman Spectra of Polyenes and Aromatics*; Spiro, T. G., Ed.; Wiley-Interscience: New York, 1987; Vol. 2, pp 1−58. (b) Myers, A. B. Excited Electronic State Properties From Ground-state Resonance Raman Intensities. In *Laser Techniques in Chemistry*; Myers, A. B., Rizzo, T. R., Eds.; Wiley: New York, 1995; pp 325−384. (c) Kelley, A. M. *J. Phys. Chem. A* **1999**, *103*, 6891−6903.

(5) Yarasi, S.; Loppnow, G. R. *J. Am. Chem. Soc.*, in press.

(6) Pan, D.; Mathies, R. A. *Biochemistry* **2001**, *40*, 7929−7936.

(7) Webb, M. A.; Fraga, E.; Loppnow, G. R. *J. Phys. Chem.* **1996**, *100*, 3278−3287.

(8) Loppnow, G. R.; Fraga, E. *J. Am. Chem. Soc.* **1997**, *119*, 895−905.

(9) Mathies, R.; Oseroff, A. R.; Stryer, L. *Proc. Natl. Acad. Sci. U.S.A.* **1976**, *73*, 1−5.

(10) Webb, M. A.; Kwong, C. M.; Loppnow, G. R. *J. Phys. Chem. B* **1997**, *101*, 5062−5069.

(11) Fraga, E.; Loppnow, G. R. *J. Phys. Chem. B* **1998**, *102*, 7659−7665.

(12) Lee, S.-Y.; Heller, E. J. *J. Chem. Phys.* **1979**, *71*, 4777−4788.

(13) Mukamel, S. *Principles of Nonlinear Optical Spectroscopy*; Oxford University Press: New York, 1995.

(14) Li, B.; Johnson, A. E.; Mukamel, S.; Myers, A. B. *J. Am. Chem. Soc.* **1994**, *116*, 11039−11047.

(15) Shoute, L. C. T.; Loppnow, G. R. *J. Chem. Phys.* **2002**, *117*, 842−850.

(16) Dobrowolski, J. C.; Rode, J. E.; Kolos, R.; Jamróz, M. H.; Bajdor, K.; Marzurek, A. P. *J. Phys. Chem. A* **2005**, *109*, 2167−2182.

(17) Lozeron, H. A.; Gordon, M. P.; Gabriel, T.; Tautz, W.; Duschinsky, R. *Biochemistry* **1964**, *3*, 1844−1850.

(18) Langer, J. J.; Wójtowicz, H.; Golankiewicz, K. *J. Photochem. Photobiol.* **1989**, *4*, 15−20.

(19) Golankiewicz, K.; Wójtowicz, H. *Pol. J. Chem.* **1986**, *60*, 943−949.

(20) Durbeej, B.; Eriksson, L. A. *J. Photochem. Photobiol. A* **2002**, *152*, 95−101.

(21) Dobrosz-Teperek, K.; Zwierzchowska, Z.; Lewandowski, W.; Bajdor, K.; Dobrowolski, J. C.; Mazurek, A. P. *J. Mol. Struct.* **1998**, *471*, 115−125.

(22) Sternglanz, H.; Bugg, C. E. *Biochim. Biophys. Acta* **1975**, *378*, 1−11.

(23) Fallon, L. *Acta Crystallogr. B* **1973**, *29*, 2549−2556.

(24) Southworth, G. R.; Gehrs, C. W. *Water Res.* **1976**, *10*, 967−971.

(25) Ishihara, H.; Wang, S. Y. *Biochemistry* **1966**, *5*, 2307−2313.

(26) Crespo-Hernández, C.; Cohen, B.; Hare, P. M.; Kolher, B. *Chem. Rev.* **2004**, *104*, 1977−2019.